Arabian Journal of Geosciences (2022) 15:1664
https://doi.org/10.1007/s12517-022-10891-z

ORIGINAL PAPER

Strengthening the surface and adsorption properties of diatomite for removal of Cr(VI) and methylene blue dye

Nady A. Fathy[1] · Sahar M. Mousa[2] · Reham M. Aboelenin[1] · Marwa A. Sherief[2] · Alaa S. Abdelmoaty[2]

Received: 3 June 2022 / Accepted: 2 October 2022 / Published online: 5 November 2022

Abstract

The main purpose of this work was to boost the surface and adsorption characteristics of diatomite (D) through chemical modifications with chitosan (DC), chitosan/titanium isopropoxide (DCTi), or chitosan/ graphene oxide (DCGr), respectively. Physicochemical characteristics of the prepared samples were investigated using SEM, TEM, XRD, FTIR, TGA, and porosity measurements. The impact of such modifiers into the D surface on the removal efficiency of chromium (VI) ions and methylene blue dye was studied in an equilibrium mode. Langmuir and Freundlich isotherms were used to analyze the adsorption data. Modifiers considerably enhanced the surface and textural properties of D through insertion of the main surface functional groups of chitosan and graphene oxide together compared to chitosan and titanium isopropoxide together or chitosan alone. In addition, the total surface area and total pore volume parameters of the unmodified D sample were improved greatly from 16.5 m^2/g, 0.036 cm^3/g to 39.8 m^2/g and 0.174 cm^3/g for DCGr, while they were 17.7 m^2/g and 0.132 cm^3/g for DC. The best adsorption results were well-defined with the Langmuir isotherm equilibrium model. Accordingly, the DCGr sample exhibited the highest uptake of Cr(VI) (about 167 mg/g) and methylene blue (66.7 mg/g). Hence, the chemical modification strategy of diatomite performed by using chitosan and graphene oxide significantly boosted the surface active sites and porosity properties and thus gave rise to the high adsorption capacity of Cr(VI) and methylene blue dye from wastewater. Hence, these findings affirmed the validity of the current strategy for surface modification of diatomite with chitosan and graphene oxide.

Keywords Diatomite · Surface modification · Adsorption · Chromium · Methylene blue dye

Introduction

Environmental protection through removal of heavy metals and organic wastes such as dyes has been the main topic of scientific research worldwide. Discharging wastewater from the mining, chrome plating, textiles, paints and pigment industries pollutes natural water sources with heavy metals and dyes, which are two groups of hazardous pollutants that have potentially antagonistic effects on humans and other species (Singh et al. 2018; Das et al. 2017; Fathy et al. 2021a). Remediation of these hazardous pollutants can be done by using a variety of techniques, such as adsorption, precipitation, membrane processes, flocculation, ion-exchange, chemical coagulation, and photo-degradation (Mallampati et al. 2015; Rathinam et al. 2017; Arshadi et al. 2014; Kwak and Lee 2018). Among them, adsorption-based technologies are widely recognized as constituting an effective and inexpensive treatment strategy for water tainted with hazardous pollutants (Singh et al. 2018; Kwak and Lee 2018). The major problem in removing extremely harmful heavy metal ions and dyes from water is how to design innovative adsorbent materials with high adsorption capacity and efficiency (Jawad and Abdulhameed 2020; Fathy et al. 2021b; Yan et al. 2015). Generally, natural clays such as bentonite, zeolite, and diatomite are cheaper than conventional adsorbents like activated carbons (Jawad and Abdulhameed

Responsible Editor: Amjad Kallel

✉ Nady A. Fathy
fathyna.77@hotmail.com

[1] Physical Chemistry Department, Research Institute of Advanced Materials Technology and Mineral Resources, National Research Centre, 33 El Bohouth Street (former Tahrir St.), Giza, Dokki P.O. 12622, Egypt

[2] Inorganic Chemistry Department, Research Institute of Advanced Materials Technology and Mineral Resources, National Research Centre, 33 El Bohouth Street (former Tahrir St.), Giza, Dokki P.O. 12622, Egypt

2020) because these clays are naturally abundant and their surfaces are easily modified (Fathy et al. 2021b). Using chitosan as a surface modifier for some adsorbent solids has attracted much attention because they are naturally available, eco-friendly, and cost-effective natural polymers (Mohamed et al. 2019; Zeng et al. 2020; Mohammad et al. 2019; Abd Malek et al. 2020; Abdulhameed et al. 2019a, b; Abdulhameed and Jawad 2020; Jawad et al. 2022). The polymeric chain of chitosan is characterized by the presence of amino ($–NH_2$) and hydroxyl (–OH) groups, which serve as potential adsorption sites for the removal of metal ions and dyes (Mohammad et al. 2019; Abd Malek et al. 2020; Abdulhameed et al. 2019a, b; Abdulhameed and Jawad 2020; Jawad et al. 2022). For instance, it has been found that modification of activated carbons with chitosan showed a better adsorption capacity for dyes (Mohamed et al. 2019) and Cr(VI) ions (Zeng et al. 2020). More recently, Jawad et al. (Mohammad et al. 2019; Abd Malek et al. 2020; Abdulhameed et al. 2019a, b; Abdulhameed and Jawad 2020; Jawad et al. 2022) pointed out modification of TiO_2 or kaolin clay with chitosan crosslinked with glyoxal, tripolyphosphate, or ethylene glycol diglycidyl ether (Mohammad et al. 2019; Abd Malek et al. 2020; Abdulhameed et al. 2019a, b; Abdulhameed and Jawad 2020; Jawad et al. 2022), which can be utilized as potentially effective adsorbents toward color dye removal. Moreover, Sabzevari et al. (2018) prepared a composite of graphene oxide (GO) crosslinked with chitosan for treatment of contaminated-water by methylene blue dye. They found that cross-linking occurs between –COOH groups of GO and amine groups of chitosan and hence exhibited superior adsorption capacity for GO-chitosan (~402 mg/g) than that of GO only (~287 mg/g).

Specifically, diatomaceous earth is an amorphous silica material formed from the remains of diatoms, which grew and were deposited in sea or lake beds. Also, it is an insulator and non-flammable, insoluble in water, and does not react with other substances in the air (Li et al. 2003). Therefore, diatomite is widely used as a filler in paints, paper, and rubber. Diatomite derived from Egypt as a natural ore of silica occurs naturally, with huge amounts in the north and west of El-Fayoum country (Ibrahim and Selim 2010; Sherief et al. 2016). The diatomaceous earth deposits in this area are generally fine-grained, friable to slightly hard rocks, and range in color from white to brownish white (Ibrahim and Selim 2010). It consists mainly of silicon dioxide (SiO_2) and some impurities such as iron, alumina, and metal oxides. Thus, there is an essential need to enhance the physicochemical properties of these materials to be used in applications such as water purification and catalysis. Accordingly, recent studies have been carried out to improve the catalytic, adsorption, and antibacterial performance of natural diatomite (Dehestaniathar et al. 2016; Gao et al. 2005; Sherief et al. 2021; Lamastra et al. 2017; Li et al. 2014; Shen et al. 2021; Aboelenin et al. 2017). For instance, a modified diatomite-supported CuO–TiO_2 composite was prepared by modification with sulfuric acid and ZrO_2 and then coated by copper and titanium oxides as catalysts in oxidation of CO (Dehestaniathar et al. 2016). Trapping of phenol from aqueous solution has been strongly improved using diatomite-modified with polyethyleneimine rather than diatomite alone because of strong electrostatic and hydrogen bond interactions (Gao et al. 2005). Very recently, diatomite was modified by depositing silver nanoparticles to induce its bioactivity as an antibacterial drug (Sherief et al. 2021). A simple and green protocol to convert the surface of hydrophobic diatomite to be slightly hydrophilic by introducing a limited content of silanol groups on the surface of diatomite and then to be silanized by bifunctional, sulfur-containing organosilanes for rubber applications was investigated (Lamastra et al. 2017).

An adsorbent material compromising porous diatomaceous earth and surface functionalized amorphous MnO_2 was reported for removing lead ions from aqueous solutions (Li et al. 2014). It was found that the adsorption capacity of diatomaceous earth for adsorbing lead ions after MnO_2 modification increased more than six times, and the adsorption of Pb(II) on the MnO_2 surface was based on the ion-exchange mechanism. Recently, Shen et al. (2021) studied the adsorption process of Cd (II) by Mn-diatomite modified adsorbent. The results have showed that the active silane chain with hydroxyl site on the diatomite matrix surface was opened and grafted by some Mn^{4+} substituted Al^{3+} ions. Compared with unmodified diatomite, the specific surface area of the adsorbent grafted with manganese oxide was increased by about eight times, and a large number of manganese hydroxyl sites were formed on its surface. Thus, the adsorption rate of Cd (II) on the modified adsorbent was increased to ~98.7%, suggesting that modified diatomite could be employed as an efficient adsorbent for the removal of Cd(II) from wastewater. Furthermore, the conversion of diatomite to mesoporous silicates supported iron oxides to perform in wet catalytic oxidation processes of methylene blue dye was investigated (Aboelenin et al. 2017). To the best of our knowledge, the modification of diatomite with chitosan only or with chitosan crosslinked with TiO_2 or GO to enhance its adsorption capacity to remove Cr(VI) and methylene blue dye from their aqueous solutions has not been studied yet.

Nevertheless, the particular aim of this work was to modify the diatomite with chitosan after heat treatment and washing with 6M HCl to remove inorganic and organic impurities and then followed by inserting either titanium isopropoxide or graphene oxide over the surface of diatomite–chitosan composite. Influencing of the chemical modification on the physicochemical properties of diatomite was carried out by tools such as SEM, TEM, XRD, FTIR, TGA,

and porosity. In order to explore the impact of these treatments, the adsorption capacities of unmodified and modified diatomite samples were estimated through equilibrium adsorption tests of chromium hexavalent ions (VI) and methylene blue dye as representative pollutants used in different industries. Therefore, the present study is considered to be a good attempt to fabricate value-added products from low-cost clays using a simple modification for environmental applications.

Experimental

Materials

Diatomaceous earth deposits were collected from the northern part of El-Fayoum Governorate, Egypt (Kom-Osheam). They consist of 69% SiO_2, 3.5% Al_2O_3, 1.75 % Fe_2O_3, some traces of other minerals (~1%), and the remaining percentage is water (Sherief et al. 2016). Sodium hydroxide pellets (NaOH, 98 %, Modern-Lab), hydrochloric acid (HCl, 37 %, Alpha-Chemika), and cetyltrimethylammonium bromide as a surfactant (CTAB, CAS# 57-09-0), acetic acid (CH_3COOH, 99%), potassium dichromate ($K_2Cr_2O_7$, 99%), and methylene blue dye ($C_{16}H_{18}ClN_3S$, CAS# 122965-43-9) were purchased from Sigma-Aldrich. Chitosan [$(C_6H_{11}NO_4)_n$, Mw= 600,000–800,000 g/mol] as a cross-linker and titanium (IV) isopropoxide ($C_{12}H_{28}O_4Ti$, 98%) as titanium source were obtained from Thermo Scientific brand of ACROS Organics. However, the graphene oxide sample was prepared from graphite flakes according to Hummer's method as reported previously by Annamalai et al. (2019).

Pretreatment of diatomite

For this purpose, an amount of diatomite was ground to powder using a mechanicalmixing grinder a mesh size (~200 nm) and then calcined at 500 ºC in air atmosphere for 3 h to remove organic components. Afterward, the calcined diatomite was treated with 6M HCl acid solution under stirring for 3 h followed by washing thoroughly with hot distilled water several times to eliminate excess acid and reduce the other inorganic residues followed by drying at 150 ºC for 5 h.

Chemical modifications

The obtained fine powder of preheated diatoms (D) in the previous step was used as a starting material through modification processes. A portion of the D sample was added into the CTAB solution to be well-dispersed before adding chitosan (0.3 g of CTAB dissolved in 15 mL of dilute acetic acid of 3 v/v% concentration) under vigorous stirring and heating at 50 ºC. Chitosan (C, 1.0 g) was dissolved in 35 mL of acetic acid (3 %), where the mass ratio of D/C was 3:1. The chitosan solution was added slowly to D dispersed in CTAB solution under stirring at 50 ºC and then the reaction was left for 60 min. After that, the product was filtered and washed with both water and ethanol then dried at 80 ºC overnight and denoted as DC. Approximately 0.25 g of titanium isopropoxide solution was weighted and diluted in 20 mL of H_2O and then poured slowly into the mixture of diatomite and chitosan as mentioned above under the same conditions. A gel form upon adding titanium isopropoxide was obtained. The mixture was filtered and washed with water/ethanol solution and then dried and denoted as DCTi. A dispersed solution of graphene oxide (5 mg in 50 mL H_2O) was added slowly to the mixture of diatoms and chitosan under the same conditions and the dried product labeled as DCGr. All the obtained solid samples were dried at 80 ºC for 3 days and then ground to powder before use.

Characterization of the prepared samples

The morphology and surface characteristics of the prepared samples were determined using a scanning electron microscope (SEM, FEI Quanta FEG-250) and high resolution-transmission electron microscope (HR-TEM, JEM-1230, Japan) operated at 120 kV. The crystalline phases in the obtained samples were determined by X-ray diffraction analysis using a Brukerdiffractometer (Bruker D8 advance, Germany). The patterns were run with CuKα1 target with a monochromator 40 kV, 40 mA. Fourier transforms infrared spectroscopy (FTIR) spectra of samples were recorded by employing a KBr pressed disc technique (2 mg of sample and 98 mg of KBr) to give the main functional groups using FTIR 6500 spectrometer (JASCO, Japan) in the range of 400–4000 cm^{-1}. Aiming to study the thermal behavior of prepared samples, thermogravimetry analysis (TG and DTG) was performed using a Shimadzu thermobalance, model TGA/DSC-50H, at a temperature range of 25–1000 ºC under N_2 atmosphere with a flow rate of 30 ml/min at heating rate of 10°/min and sample mass of 5 mg. Also, the textural properties such as Brunauer–Emmett–Teller (BET) surface area (S_{BET}, m^2/g), total pore volume (V_p, cm^3/g), and average pore diameter (R_p, nm) were measured using nitrogen adsorption analysis at –196 ºC (BEL-Sorp-max, MicrotracBel Crop, Japan).

Liquid phase adsorption experiments

Batch adsorption experiments were carried out toward both adsorbates; i.e., hexavalent chromium (Cr(VI)) and methylene blue dye of separate solutions to study the adsorption capacity of the unmodified and modified diatomite samples. Approximately 20 mL of adsorbate solutions with different initial concentrations (20–100 mg/L) were used with 20 mg

of adsorbent under shaking at 200 rpm and 25 ºC for 24 h. The dye concentrations in the filtrate were determined using a UV-visible spectrophotometer (Shimadzu Model PC-2401) with 1.0 cm length–path cell by measuring the maximum absorbance at a wavelength of 642 nm for methylene blue dye and 540 nm for Cr(VI) after complexation of Cr(VI) with diphenylcarbazide indicator as described previously (Fathy et al. 2021a).

Adsorption calculations

The adsorbed amount of adsorbate (Cr(VI) or methylene blue dye) was calculated from the mass balance expression given by:

$$q_e = \frac{(C_o - C_e)}{\mathrm{m}} V \tag{1}$$

where q_e is the amount of adsorbate by the adsorbents (mg/g), C_o initial ion concentration of adsorbate (mg/L), C_e equilibrium concentration of adsorbate (mg/L), m the mass of adsorbent in (mg), and V is the volume of metal solution in contact with the adsorbent (mL). Langmuir and Freundlich isotherm models (Langmuir 1918; Freundlich 1906), as well-known adsorption isotherms, were used. These models are presented in the following equations:

Langmuir isotherm (Langmuir 1918):

$$\frac{\mathrm{C_e}}{\mathrm{q_e}} = \frac{1}{\mathrm{K_L Q}} + \frac{1}{\mathrm{Q}}\mathrm{C_e} \tag{2}$$

where Q is the maximum adsorption capacity (mg/g) and $\mathrm{K_L}$ (L/mg) is the Langmuir adsorption equilibrium constant Q, and $\mathrm{K_L}$ are calculated from the slope and intercept of the isotherm plot $\mathrm{C_e/q_e}$ versus $\mathrm{C_e}$, respectively.

The essential characteristic of the Langmuir isotherm can be expressed in terms of a dimensionless constant called equilibrium parameter:

$$R_L = \frac{1}{1 + C_o K_L} \tag{3}$$

where $\mathrm{C_o}$ is the highest initial dye concentration (mg/L). The value of $\mathrm{R_L}$ indicates the type of isotherm to be either favorable ($0 < \mathrm{R_L} < 1$), linear ($\mathrm{R_L} = 1$), unfavorable ($\mathrm{R_L} > 1$), or irreversible ($\mathrm{R_L} = 0$).

Freundlich isotherm (Freundlich 1906):

$$\ln\ q_e = \ln\ K_F + \frac{1}{n} \ln\ C_e \tag{4}$$

where $\mathrm{K_F}$ is the Freundlich isotherm constant (mg/g(mg/L)$^{1/n}$), which is an indicator of the adsorptive capacity of an adsorbent fora solute, and n is a measure of the intensity of the adsorption or surface heterogeneity (a value closer to zero for 1/n represents a moreheterogeneous surface); however, the Freundlich exponent, n, should have values lying in the range of 1 to 10 for classification as a preferable adsorption.

Quality control

All experiments were carried out in duplicate measurements to calculate the relative standard deviations (RSD). RSD values were found to be less than 5% within all experiments.

Results and discussion

Properties of modified diatoms by SEM and TEM investigations

Figure 1 shows the surface characteristics of the starting preheated diatomite (i.e., unmodified) and their corresponding modified samples as evident by SEM images. Figure 1A indicates the frustules structure of diatomite consisting of large silica grains with open cavities on its roughness surface. Also, a set of irregular arrays of rectangular pores along the tubes can be seen. In Fig. 1B, it was observed that the chitosan molecules that contain several amino and hydroxyl groups as active sites covered cavities and arrays on diatomite surface (Jawad et al. 2022; Sabzevari et al. 2018), which would increase the interaction with the additional species of titanium isopropoxide or –COOH groups of graphene oxide (Sabzevari et al. 2018). Thus, considerable surface changes occurred when titanium and graphene oxide molecules were added to modify the surface of DC sample, as shown in Fig. 1C and D.

TEM images of the prepared samples are shown in Fig. 2. Clearly, the morphology of unmodified diatomite reveals an aggregation of silica particles as spherical shape (Fig. 2A). Through modification, the CTAB surfactant was used to enhance the surface activity between the diatomite particles and chitosan, as seen in Fig. 2B. Probably the chitosan molecules as a good cross-linker could enhance interlinkage with both Ti–O–Ti of titanium isopropoxide and –COOH groups of graphene oxide molecules over the DC sample, as shown in Fig. 2C and D. This result is in agreement with previous studies on chitosan–tripolyphosphate/kaolin clay composite (Abdulhameed and Jawad 2020). Furthermore, graphene oxide sheets are found to be loosely stacked layers that have covered the whole surface of the DC sample due to crosslinking bonds between COOH groups of graphene and $–NH_2$ groups of chitosan covered diatomite surface (Sabzevari et al. 2018).

Figure 3 illustrates the XRD profiles of the investigated samples. The XRD profile of D shows that the material is slightly amorphous, where somewhat crystalline phases

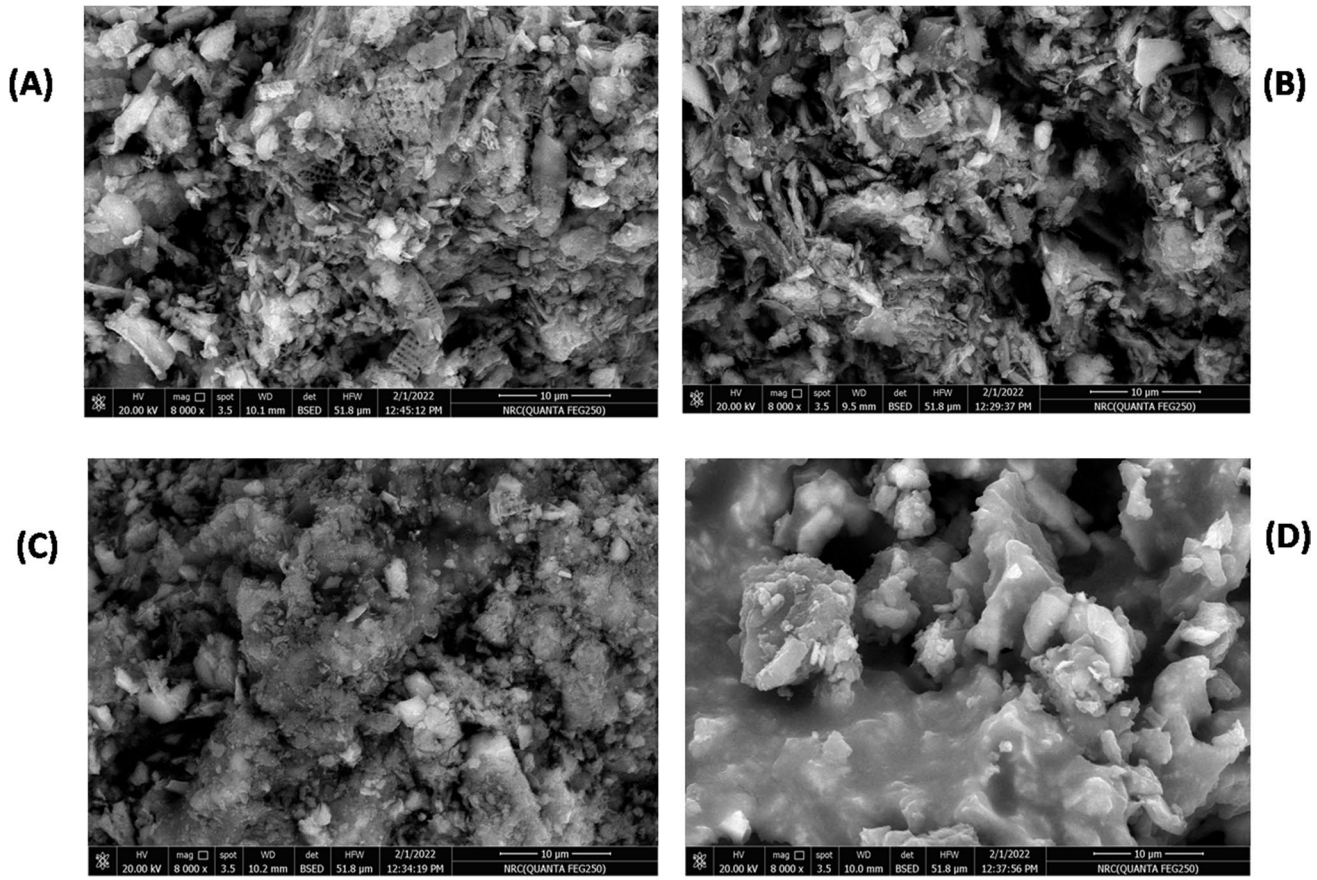

Fig. 1 SEM images of (**A**) D, (**B**) DC, (**C**) DCTi, and (**D**) DCGras-prepared samples

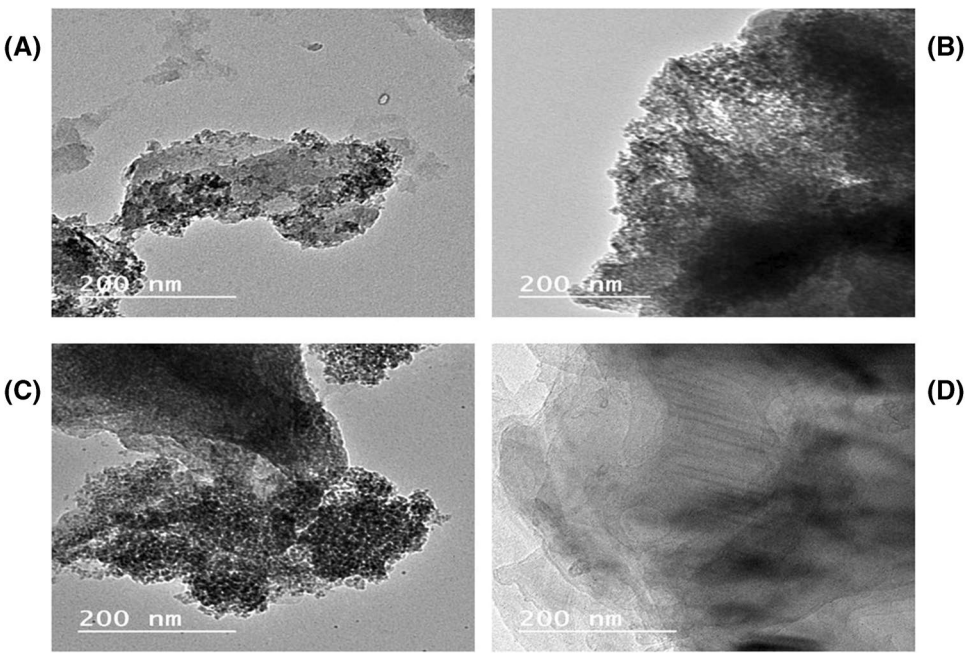

Fig. 2 TEM images of (**A**) D, (**B**) DC, (**C**) DCTi, and (**D**) DCGras-prepared samples

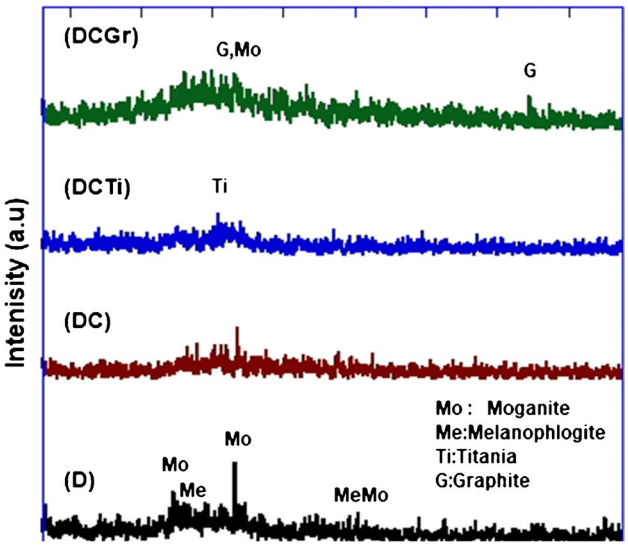

Fig. 3 XRD profiles of the prepared samples

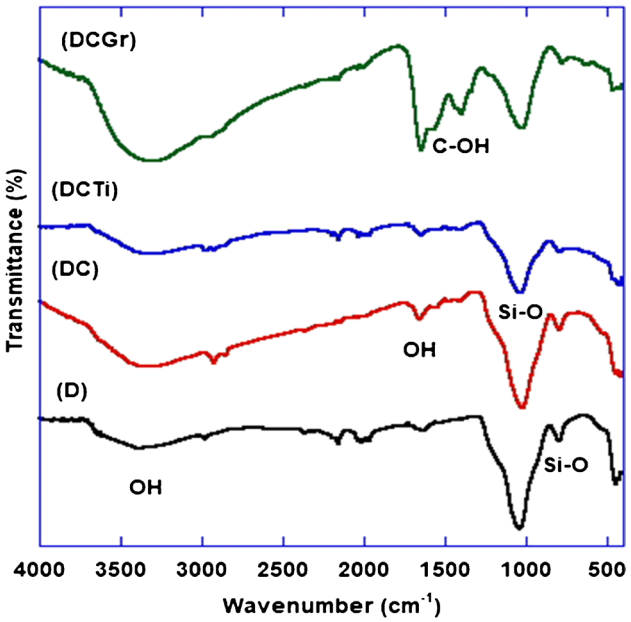

Fig. 4 FTIR spectra of D, DC, DCTi, and DCGr samples

appear. The main phases are found to be polymorphs of quartz called moganite (JCPDS#64-1441) and melanophlogite (JCPDS#16-0331) as SiO_2 in a monoclinic crystal system (Lee et al. 2021). The intensity of the crystalline phase of moganite was reduced after modification of D with chitosan confirming that the surface interconnection between diatomite and chitosan molecules occurred. A phase of titanium oxide as anatase type (JCPDS#89-4921) is formed as depicted in XRD patterns of DCTi (Reddy et al. 2015). A typical XRD pattern of graphite peak at 2θ of 26° (002) (JCPDS#02-0456) in XRD of DCGr is obtained (Ji et al. 2012). Thus, the obtained results can confirm that the surface changes obtained through modification of diatomite/chitosan (DC) with titanium isopropoxide and graphene oxides molecules under stirring at 50 ºC for 60 min could significantly enhance the surface properties of unmodified diatomite (D).

Considering the change in the functional groups on the surface of modified samples through modification treatments, the FTIR spectra for the D, DC, DCTi, and DCGr samples were recorded as shown in Fig. 4. The spectrum of D shows the transmittance at 454 cm^{-1} which represents the Si–O–H stretching vibration, while the one between 900–1067 cm^{-1} signifies the Si–O–Si stretching vibration (Jawad and Abdulhameed 2020; Jawad et al. 2022; Dehestaniathar et al. 2016; Gao et al. 2005; Sherief et al. 2021; Lamastra et al. 2017; Li et al. 2014; Shen et al. 2021). The band around 3433 cm^{-1} corresponds to the vibration of N–H and –OH groups coordinated by hydrogen bonding (Zeng et al. 2020; Mohammad et al. 2019; Abd Malek et al. 2020; Abdulhameed et al. 2019a, b; Abdulhameed and Jawad 2020; Jawad et al. 2022; Sabzevari et al. 2018). Upon addition of chitosan, two shoulder bands at 2921 and 2850 cm^{-1} occur due to symmetric and asymmetric C–H stretching in the CH_3 group confirming the presence of chitosan (Zeng et al. 2020; Mohammad et al. 2019; Abd Malek et al. 2020; Abdulhameed et al. 2019a, b; Abdulhameed and Jawad 2020; Jawad et al. 2022). Moreover, a shoulder band at 1634 cm^{-1} is due to N–H bending vibration of $–NH_2$ groups (Sabzevari et al. 2018). The absorption peak of Si–O–Si related to silicate in diotamite is reduced upon addition of chitosan, titanium isopropoxide, and graphene oxide molecules, successively. In the spectrum of DCGr, two distinctive absorption peaks are formed. The band at the vicinity of 1720 cm^{-1} is attributed to the absorption of carboxylic acid and/or the carbonyl stretching vibration of C=O, which is attributed to –COOH and C=O in the surface and/or edge and of the graphene oxide. The band observed at 1380 cm^{-1} is the stretching vibration of the epoxy groups (C–O–C) and carboxyl C–O in graphene oxide (Sabzevari et al. 2018; Annamalai et al. 2019). The broadness of the absorption band at 3433 cm^{-1} is increased in the FTIR spectrum of DCGr as compared to that of DC confirming the cross-linking of –COOH groups of the graphene oxide surface into $–NH_2$ of the DC matrix. All above-mentioned results indicate that D sample was successfully modified with chitosan and then with graphene oxide, which is abundant in hydrophilic oxygen-containing groups which would considerably enhance the adsorption capacity for DC.

Figure 5 shows the thermal properties of the prepared samples. All samples show different mass loss with increasing temperature from 25 to 1000 ºC. Data of DTG peaks showing temperatures accompanied with mass loss are very different, and there are three thermal stages. In the first stage,

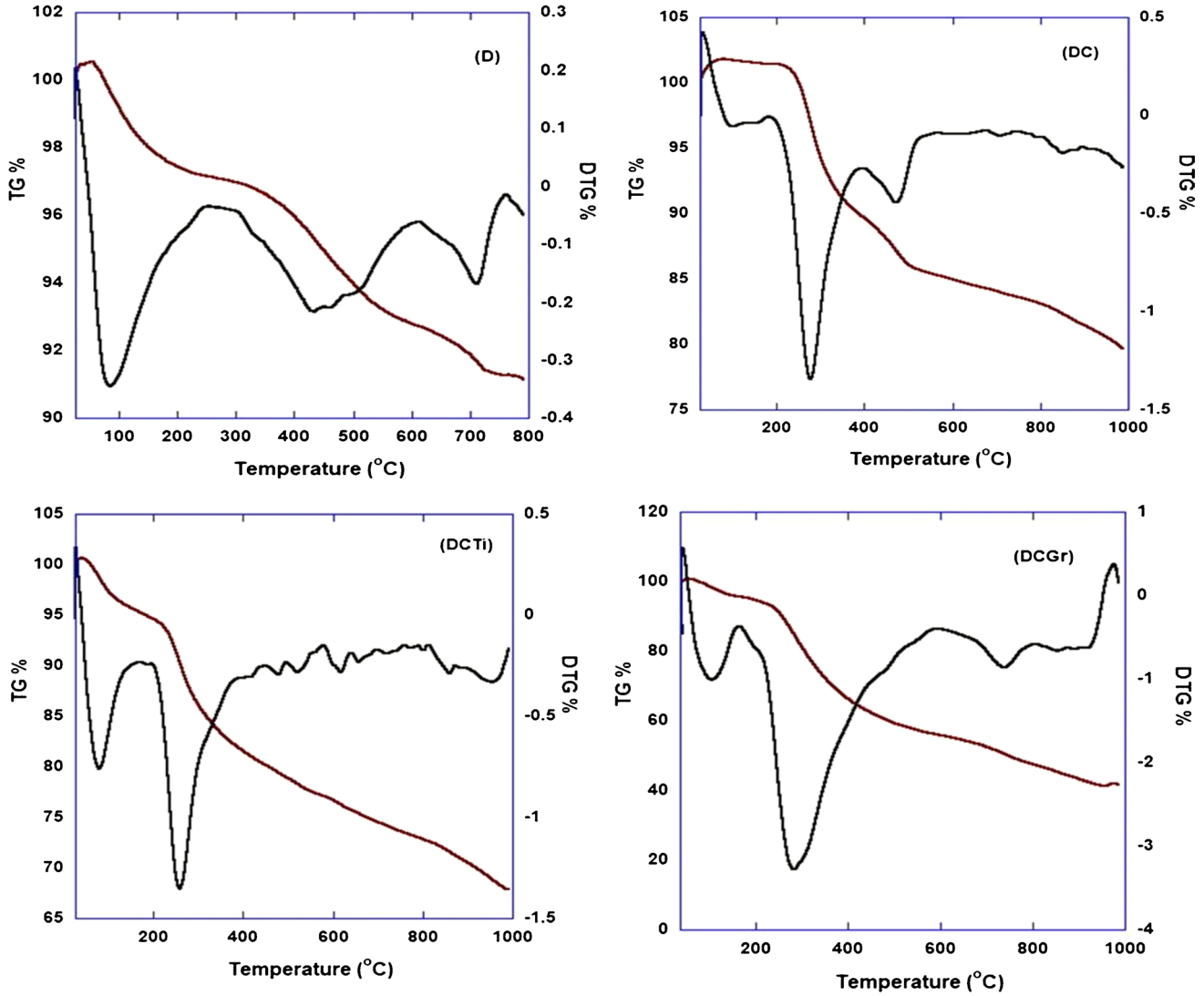

Fig. 5 TGA profiles of the prepared samples

the peak centered at 50 to 100 ℃ is assigned to the loss of water absorbed on the diatomite. After that, the peak appearing between 250 to 430°C might be due to the liberation of water caused by dehydroxylation of some associated silanol groups on the external surface of the diatomite. At the high temperature region, the third stage between 520–780 °C has been ascribed to a formation of siloxane bridges resulting from dehydroxylation of isolated silanol groups on the internal surface of the diatomite (Goren et al. 2002). As a result of the evaporation, new voids and defects may occur forming the amorphous structure in the modified samples. The percentages of mass loss were found to be 8, 22, 33, and 60% for D, DC, DCTi, and DCGr samples.

The textural features of samples were evaluated using the N_2 physisorption analyzer. The Brunauer, Emmett, and Teller method (BET) was employed to assess the specific surface area (S_{BET}, m^2/g), total pore volume (V_P, cm^3/g), and average pore diameter ($_{RP}$, nm), as listed in Table 1. It can be seen that the applied modifications on the diatomite surface can reflect an increase in both total surface area and total pore volume with a decrease in average pore volume.

Table 1 Porous characteristics of the prepared samples as accounted from the BET method and slurry pH of samples

Samples	S_{BET} (m^2/g)	V_P (cm^3/g)	$_{RP}$ (nm)	Pore size distribution (nm)	Slurry pH
D	16.5	0.0364	104.9	15.9	4
DC	17.7	0.132	29.8	11.3	5
DCTi	29.9	0.126	7.40	5.07	4
DCGr	39.8	0.174	16.6	8.30	8

Nevertheless, the modification of diatomite with both chitosan and graphene can boost the internal porosity. Obviously, the DCGr sample exhibited the largest BET surface area and total pore volume as compared with the counterpart sample DC (cf. Table 1). In addition, the DCGr sample is the richest in containing acidic oxygen functional groups as coincided by FTIR analysis. From these results, it can be concluded that this modification strategy significantly enhances the surface and porosity properties of diatomite.

Adsorption studies of Cr(VI)

The contamination of chromium in wastewater streams produced from various operations of electroplating, tanneries, and mining is of great concern because it has dangerous impacts on human health and aquatic organisms when the concentrations reach above those limited by law. Chromium can exist in nine valence states starting from –2 to +6. However, the most stable oxidation forms are hexavalent chromium (Cr(VI)) and trivalent chromium (Cr(III)) species (Singh et al. 2018; Das et al. 2017; Fathy et al. 2021a; Ammar et al. 2021).

The adsorption of Cr(VI) by the unmodified and modified diatomite was analyzed using Langmuir and Freundlich isotherms, and their corresponding data are summarized in Table 2. Figure 6A depicts the adsorption isotherms for Cr(VI) onto D and DCGr samples as an example with their analyzed data by Freundlich isotherm (Fig. 6B). Results indicated that the correlation coefficient values (R^2) calculated from the Freundlich isotherm is higher than that of the Langmuir isotherm confirming that adsorption is well-fitted by the Freundlich model. This finding suggests the formation of more heterogeneous sites due to the surface modification. The unmodified diatomite D sample showed the lowest adsorption capacity (8.22 mg/g), whereas the modified D with chitosan and graphene oxide exhibited the highest capacity (167 mg/g). There is an increase of about 91% upon addition of chitosan and 67% when graphene oxide is intercalated into the DC sample. This enhancement in the monolayer adsorption capacity (Q, mg/g) is attributed mainly to high total surface area, total pore volume, and reachable oxygen functional groups that uptake Cr(VI) ions obtained upon addition of graphene oxide.

Table 2 Equilibrium parameters derived from Langmuir and Freundlich isotherms for adsorption of Cr(VI) onto the prepared materials at pH 3.5 and 25 ºC

Models	D	DC	DCTi	DCGr
Langmuir				
Q (mg/g)	8.22	100	53	167
K_L *(L/g)*	0.837	0.042	0.034	0.027
R^2	0.669	0.918	0.909	0.919
Freundlich				
K_F *((mg/g)/(L/mg)$^{1/n}$)*	2.38	6.28	4.98	6.17
1/n	1.041	0.634	0.474	0.732
R^2	0.842	0.954	0.939	0.978

Adsorption studies of MB dye

Methylene blue dye (MB) is one of the most recognized probe molecules and frequently mentioned in the technical specifications of activated carbons (Attia et al. 2008; Girgis et al. 2011). The fitting parameters of Langmuir and Freundlich models are given in Table 3, and the applicability was evaluated by using the correlation coefficients (R^2). Figure 7A depicts the adsorption isotherms for MB dye onto D and DCGr samples as an example with their analyzed data by Freundlich isotherm (Fig. 7B). The results indicate that the two models can fit the experimental data well. The maximum adsorption capacity derived from the Langmuir isotherm increases approximately 22 times after modification with chitosan and graphene oxide. Therefore, the DCGr sample can efficiently remove MB dye from aqueous solutions confirming the validity of modification.

Table 4 summarizes a comparison of adsorption capacity of Cr(VI) and MB dye by various adsorbents in the literature (Fathy et al. 2021a; Mallampati et al. 2015; Jawad and

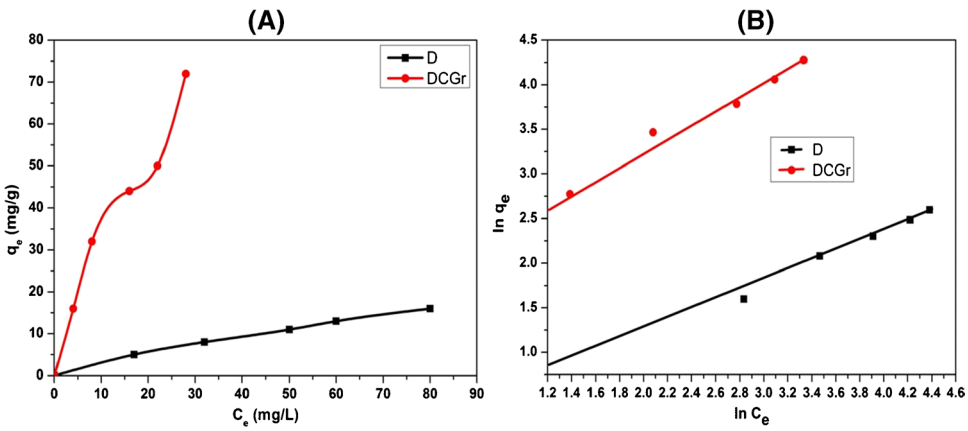

Fig. 6 **A** Adsorption isotherms and **B** Freundlich plots for of adsorption Cr(VI) onto D and DCGr samples

Table 3 Calculated parameters from Langmuir and Freundlich isotherms for adsorption of MB dye at pH 6 and 25 ℃

Models	D	DC	DCTi	DCGr
Langmuir				
Q (mg/g)	3.41	30.3	26.3	66.7
K_L *(L/g)*	0.937	0.119	0.165	0.175
R^2	0.888	0.941	0.971	0.984
Freundlich				
K_F *((mg/g)/(L/mg)$^{1/n}$)*	2.38	10.3	8.57	11.4
1/n	1.54	0.218	0.254	0.547
R^2	0.962	0.954	0.974	0.997

Abdulhameed 2020; Zeng et al. 2020; Fengxi et al. 2016; Ebrahimi and Kumar 2021; Allam et al. 2018; Altun 2020; Moussout et al. 2018). Taking into consideration the surface properties of each adsorbent, it has been found that the best adsorbent prepared in this study (DCGr) has a higher adsorption capacity toward Cr(VI) than toward MB dye as compared to other adsorbents.

Conclusions

The current study successed to developed a strategy for boosting the surface and adsorption properties of natural diatomite to remove Cr(VI) and methylene blue dye from their aqueous solutions. A novel attempt was made to prepare efficient adsorbents of diatomite by integrating nanocrystals with the porous matrix of titanium isopropoxide and graphene oxide into diatomite modified with chitosan. The materials were characterized using SEM, TEM, XRD, FTIR, TGA, and porosity measurements to affirm the changes in physicochemical properties of unmodified diatomite (D). Based on the obtained results from the applied analyses, the morphology and surface properties of the D sample were enhanced notably after crosslinking with either chitosan or chitosan with graphene oxide comparing to that of chitosan with titanium isopropoxide. The combination of chitosan groups and graphene oxide sheets on the D surface led to enhancement in the surface groups and textural properties of D. The presence of acidic oxygen functional groups and high total surface area of the DCGr sample significantly improved the adsorption efficiency toward Cr(VI) ions and MB dye from wastewater. The

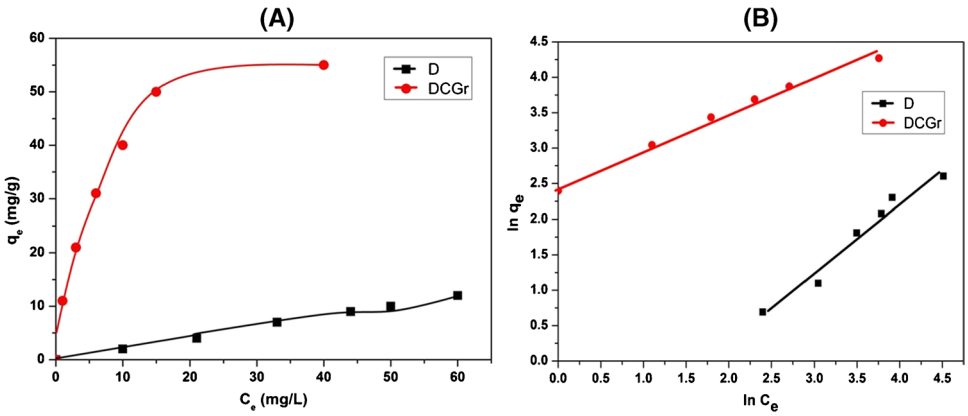

Fig. 7 **A** Adsorption isotherms and **B** Freundlich plots for adsorption MB dye onto D and DCGr samples

Table 4 Comparison of the adsorption capacity (Q, mg/g) of Cr(VI) and MB dye by various adsorbents

Adsorbents	Q, mg/g Cr(VI)	Q, mg/g MB dye	Ref.
Modified carbon nanostructures	44–56 (25 ℃)	–	(Fathy et al. 2021a)
Fruit peels	–	62 (30 ℃)	(Mallampati et al. 2015)
Mesoporous Iraqi red kaolin	–	240 (30 ℃)	(Jawad and Abdulhameed 2020)
Activated carbon coated with chitosan	21.8 (30 ℃)	–	(Zeng et al. 2020)
Chinese diatomite	–	15.1	(Fengxi et al. 2016)
Modified diatomite	–	127	(Ebrahimi and Kumar 2021)
Activated Moroccan clay	–	50	(Allam et al. 2018)
Chitosan coated bentonite clay	106.4 (25 ℃)	–	(Altun 2020)
Chitosan/Zeolite film	17.3 (25 ℃)	–	(Moussout et al. 2018)
DCGr	167 (25 ℃)	66.7 (25 ℃)	**This study**

monolayer adsorption capacity (Q, mg/g) of the GO-LCTS material with Cr(VI) was 167 mg/g and with MB dye was 66.7 mg/g. The Langmuir isotherm model, which suggests monolayer adsorption at the binding sites on the surface of the adsorbent and adsorbates and is dominated by electrostatic interaction, proved helpful in explaining the adsorption process of Cr(VI) and MB dye adsorbates. Overall, this work demonstrates the potential utility of the diatomite–chitosan–graphene oxide composite as a talented adsorbent in the solid–liquid phase adsorption and for potential applications in wastewater decontamination.

Acknowledgment The authors are thankful to the National Research Center, Egypt for supporting this work with technical facilities, including chemicals and equipments.

Author's contributions All the authors contributed equally in this work. All authors contributed to the study conception and design. Material preparation, data collection and analysis were performed 70% by Nady Fathy, Sahar Mousa, Reham Aboelenin and 30% by Marwa Sherief and Alaa Abdelmoaty. Writing – original draft was by Nady Fathy and review and editing by Sahar Mousa. Both Reham Aboelenin and and Marwa Sherief commented on and edited the first draft. All authors read and approved the final manuscript.

Funding Open access funding provided by The Science, Technology & Innovation Funding Authority (STDF) in cooperation with The Egyptian Knowledge Bank (EKB). The authors have not received any specific financial funding for this work.

Declarations

Conflict of interest The authors declare that they have no competing interests.

References

Abd Malek NN, Jawad AH, Abdulhameed AS (2020) New magnetic Schiff's base-chitosan-glyoxal/fly ash/Fe_3O_4 biocomposite for the removal of anionic azo dye: an optimized process. Int J Biol Macromol 146:530–539

Abdulhameed AS, Jawad AH (2020) Facile synthesis of crosslinked chitosan-tripolyphosphate/kaolin clay composite for decolourization and COD reduction of remazol brilliant blue R dye: optimization by using response surface methodology. Coll Surf A: Physicochem Eng Aspects 605:125329

Abdulhameed AS, Mohammad AT, Jawad AH (2019a) Application of response surface methodology for enhanced synthesis of chitosan tripolyphosphate/TiO_2 nanocomposite and adsorption of reactive orange 16 dye. J Clean Prod 232:43–56

Abdulhameed AS, Jawad AH, Mohammad AT (2019b) Synthesis of chitosan-ethylene glycol diglycidyl ether/TiO_2 nanoparticles for adsorption of reactive orange 16 dye using a response surface methodology approach. Bioresour Technol 293:122071

Aboelenin RMM, Fathy NA, Farag HK, Sherief MA (2017) Preparation, characterization and catalytic performance of mesoporous silicates derived from natural diatomite: comparative studies. J Water Process Eng 19:112–119

Allam K, Gourai K, EL Bouari A, Belhorma B, Bih L (2018) Adsorption of methylene blue on raw and activated Clay: case study of Bengurir clay. J Mater Environ Sci 9:1750–1761

Altun T (2020) Preparation and application of glutaraldehyde crosslinked chitosan coated bentonite clay capsules: chromium (VI) removal from aqueous solution. J Chil Chem Soc 65:4790–4797

Ammar NS, Fathy NA, Ibrahim HS, Mousa SM (2021) Micro-mesoporous modified activated carbon from corn husks for removal of hexavalent chromium ions. Appl Water Sci 11(154):1–12

Annamalai KP, Zheng X, Gao J, Chen T, Tao Y (2019) Nanoporous ruthenium and manganese oxide nanoparticles/reduced graphene oxide for high-energy symmetric supercapacitors. Carbon 144:185–192

Arshadi M, SalimiVahid F, Salvacion JWL, Soleymanzadeh M (2014) Adsorption studies of methyl orange on an immobilized Mn-nanoparticle: kinetic and thermodynamic. RSC Adv 4:16005–16017

Attia AA, Girgis BS, Fathy NA (2008) Removal of methylene blue by carbons derived from peach stones by H_3PO_4 activation: batch and column studies. Dyes Pigments 76:282–289

Das B, Sharma M, Sarmah JC, Bania KK (2017) Rapid reduction of dye pollutants and hexavalent chromium by silver-sulphur oxido-vanadium cluster. J Environ Chem Eng 5:4212–4219

Dehestaniathar S, Khajelakzay M, Ramezani-Farani M, Ijadpanah-Saravi H (2016) Modified diatomite-supported CuO–TiO_2 composite: preparation, characterization and catalytic CO oxidation. J Taiwan Inst Chem Eng 58:252–258

Ebrahimi P, Kumar A (2021) Diatomite chemical activation for effective adsorption of methylene blue dye from model textile wastewater. Intern J Environ Sci Develop 12:23–28

Fathy NA, El-Khouly SM, El-Shafey O (2021a) Modified carbon nanostructures obtained from sugarcane bagasse hydrochar for treating chromium-polluted water, Current. Anal Chem 17:975–988

Fathy NA, El-Khouly SM, Ahmed SAS, El-Nabarawy TA, Tao Y (2021b) Superior adsorption of cationic dye on novel bentonite/carbon composites. Asia Pac J Chem Eng 16:e2586

Fengxi W, Peijun N, Zhangmin L, Xiangyun D (2016) Comparison on adsorption of methylene blue using frustules and diatomite, Chinese. J Environ Eng 10:1693–1698

Freundlich HMF (1906) Over the adsorption in solution. J Phys Chem 57:385–470

Gao B, Jiang P, An F, Zhao S, Ge Z (2005) Studies on the surface modification of diatomite with polyethyleneimine and trapping effect of the modified diatomite for phenol. Appl Surf Sci 250:273–279

Girgis BS, Soliman AM, Fathy NA (2011) Development of micro mesoporous carbons from several seed hulls under varying conditions of activation. Microporous Mesoporous Mater 142:518–525

Goren R, Baykara F, Marsoglu M (2002) A study on the purification of diatomite in hydrochloric acid. Scand J Metall 31:115–119

Ibrahim SS, Selim AQ (2010) Producing a micro-porous diatomite by a simple classification process. J Ore Dressing 12:25–33

Jawad AH, Abdulhameed AS (2020) Mesoporous Iraqi red kaolin clay as an efficient adsorbent for methylene blue dye: Adsorption kinetic, isotherm and mechanism study. Surf Interf 18:100422

Jawad AH, Abdulhameed AS, Kashi E, Yaseen ZM, ALOthman ZA, Khan MR (2022) Cross-linked chitosan-glyoxal/kaolin clay composite: parametric optimization for color removal and COD reduction of remazol brilliant blue R dye. J Polym Environ 30:164–178

Ji Z, Zhu G, Shen X, Zhou H, Wu C, Wang M (2012) New J Chem 36:1774. https://doi.org/10.1039/c2nj40133a

Kwak HW, Lee KH (2018) Polyethylenimine-functionalized silk sericin beads for high-performance remediation of hexavalent chromium from aqueous solution. Chemosphere 207:507–516

Lamastra FR, Mori S, Cherubini V, Scarselli M, Nanni F (2017) A new green methodology for surface modification of diatomite filler in elastomers. Mater Chem Phys 194:253–260

Langmuir I (1918) The adsorption of gases on plane surfaces of glass, mica and platinum. J Am Chem Soc 40:1361–1403

Lee S, Xu H, Xu H, Neuefeind J (2021) Crystal structure of moganite and Its anisotropic atomic displacement parameters determined by synchrotron X-ray diffraction and X-ray/neutron pair distribution function analyses. Minerals 11:272

Li X, Bian C, Chen W, He J, Wang Z, Xu N, Xue G (2003) Polyaniline on surface modification of diatomite: a novel way to obtain conducting diatomite fillers. Appl Surf Sci 207:378–383

Li S, Li D, Su F, Ren Y, Qin G (2014) Uniform surface modification of diatomaceous earth with amorphous manganese oxide and its adsorption characteristics for lead ions. Appl Surf Sci 317:724–729

Mallampati R, Xuanjun L, Adin A, Valiyaveettil S (2015) Fruit peels as efficient renewable adsorbents for removal of dissolved heavy metals and dyes from water. ACS Sustain Chem Eng 3:1117–1124

Mohamed GM, Rashwan WE, Fathy NA, Ahmed SAS (2019) Effect of nitrogen functionalization on the adsorption performance of commercial charcoal activated with phosphoric acid. Des Water Treat 148:178–187

Mohammad AT, Abdulhameed AS, Jawad AH (2019) Box-Behnken design to optimize the synthesis of new crosslinked chitosan-glyoxal/TiO_2 nanocomposite: methyl orange adsorption and mechanism studies. Int J Biol Macromol 129:98–109

Moussout H, Ahlafi H, Aazza M, El Akili C (2018) Performances of local chitosan and its nanocomposite 5%Bentonite/Chitosan in the removal of chromium ions (Cr(VI)) from wastewater. Int J Biol Macromol 108:1063

Rathinam K, Singh SP, Li Y, Kasher R, Tour JM, Arnusch CJ (2017) Polyimide derived laser-induced graphene as adsorbent for cationic and anionic dyes. Carbon 124:515–524

Reddy KR, Hassan M, Gomes VG (2015) Hybrid nanostructures based on titanium dioxide for enhanced photocatalysis. Appl Catal A Gen 489:1–16

Sabzevari M, Cree DE, Wilson LD (2018) Graphene oxide−chitosan composite material for treatment of a model dye effluent. ACS Omega 3:13045–13054

Shen T, Xu H, Miao Y, Ma L, Chen N, Xie Q (2021) Study on the adsorption process of Cd(II) by Mn-diatomite modified adsorbent. Mater Lett 300:130087

Sherief MA, Hanna AA, Abdelmoaty AS (2016) Studies on the effect of diatomite on the flammability of ammonium polyphosphate/polypropylene. Intern J Chem Tech Res 9:822–830

Sherief MA, El-Bassyouni GT, Gamal AA, Esawy MA (2021) Modification of diatom using silver nanoparticle to improve antimicrobial activity. Mater Today: Proceed 43:3369–3374

Singh SP, Rathinam K, Kasher R, Arnusch CJ (2018) Hexavalent chromium ion and methyl orange dye uptake via a silk protein sericin–chitosan conjugate. RSC Adv 8:27027–27036

Yan L-g, Qin L-L, Yu H-Q, Li S, Shan R-R, Du B (2015) Adsorption of acid dyes from aqueous solution by CTMAB modified bentonite: Kinetic and isotherm modeling. J Mol Liq 211:1074–1081

Zeng G, Hong C, Zhang Y, You H, Shi W, Du M, Ai N, Che B (2020) Adsorptive removal of Cr(VI) by Sargassum horneri–based activated carbon coated with chitosan. Water Air Soil Pollut 231:1–12